JOURNAL OF APPLIED CRYSTALLOGRAPHY
ISSN 1600-5767

The RAPTR furnace: a rapid heating and cooling sample furnace for *in situ* X-ray scattering studies of temperature-induced reactions. Corrigendum

Danrui Hu,[a]‡ Michelle L. Beauvais,[a]‡ Bryce G. Mullens,[b] Bryan A. Sanchez Monserrate,[a] Simon M. Vornholt,[a] Gabrielle E. Kamm,[a] John J. Ferrari,[a] Peter J. Chupas[a] and Karena W. Chapman[a]*

[a]Department of Chemistry, Stony Brook University, 100 Nicolls Road, Stony Brook, NY 11790-3400, USA, and [b]School of Chemistry, University of Sydney, Sydney, New South Wales 2006, Australia. *Correspondence e-mail: karena.chapman@stonybrook.edu

Received 23 January 2026
Accepted 23 March 2026

Edited by S. Moggach, The University of Western Australia, Australia

‡ These authors contributed equally.

Keywords: sample environments; *in situ* X-ray scattering; solid-state reactions; kinetics; high temperature.

Supporting information: this article has supporting information at journals.iucr.org/j

Errors in the article by Hu *et al.* [*J. Appl. Cryst.* (2024), **57**, 88–93] are corrected.

For the article by Hu *et al.* (2024), errors in the structural models fitted to the diffraction data for an example solid-state reaction are corrected. The corrections are confined to Section 5 of that article, which illustrates an application of the RAPTR furnace. A revised version of this section is provided below, together with the corrected Fig. 6.

For the reaction of PbO and WO_3, the WO_3 polymorph present at the reaction temperature was incorrectly modelled as the β polymorph rather than α-WO_3. In addition, the reaction intermediate was misidentified as Pb_3WO_6 instead of Pb_2WO_5. These errors affected the quantitative phase analysis, reported reaction evolution and mechanistic details.

5. Capturing the fast solid-state reaction of PbO and WO_3

The synthesis of the scheelite-type $PbWO_4$ was evaluated as a model stoichiometric solid-state reaction ($PbO + WO_3 \rightarrow PbWO_4$). Traditionally, scheelite-type oxides are synthesized via conventional solid-state synthesis routes, heating in air at high temperatures (700–900°C) for long time periods (>2 h) (Mullens *et al.*, 2023). Both Pb and W are heavy elements, and as such are expected to be relatively immobile, such that a slow reaction would be anticipated. An initial test reaction undertaken *ex situ* by heating a stoichiometric mixture of PbO (Puratronic, 99.999%) and WO_3 (NanoAmor, 99.9+%) at 750°C in air in a muffle furnace for 12 h yielded scheelite-type $PbWO_4$ as a phase-pure product.

Stoichiometric quantities of reagents were mixed and formed into pellets (~70% packing density) to optimize contact between particles, before loading into the 1.1 mm OD SiO_2 glass capillary (Kamm *et al.*, 2022). Capillary-loaded reaction mixtures were assembled within the RAPTR furnace, and fast time-resolved X-ray diffraction data were collected at beamline 11-ID-B of the Advanced Photon Source at Argonne National Laboratory ($\lambda = 0.2116$ Å, sample-to-detector distance $\simeq 1.0$ m) following translation of the mixture into the hot zone at 750°C. Data were collected with 1 s

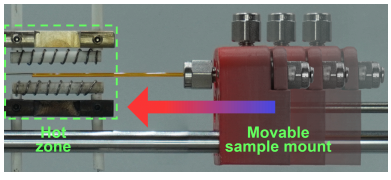

exposures during the first minute following translation, and then at increasing intervals at longer times: 2 s exposures (1–2 min), 5 s exposures (2–4 min), 10 s exposures (4–6 min), 30 s exposures (6–10 min), matching the data density to the anticipated rate of change for the reaction.

The time-resolved *in situ* diffraction data acquired following rapid heating to initiate the reaction using the RAPTR furnace showed that the solid-state synthesis of $PbWO_4$ proceeds *via* three steps (Fig. 1):

$$PbO + WO_3 \rightarrow \text{Pb-rich } PbO{-}WO_3 \text{ melt} + WO_3,$$

$$\text{Pb-rich } PbO{-}WO_3 \text{ melt} + WO_3 \rightarrow \tfrac{1}{2}Pb_2WO_5 + \tfrac{1}{2}WO_3,$$

$$\tfrac{1}{2}Pb_2WO_5 + \tfrac{1}{2}WO_3 \rightarrow PbWO_4.$$

At room temperature, a three-phase mixture of α-PbO (*P*4/*nmm*, $a \simeq 3.9$ Å, $c \simeq 5.0$ Å), β-PbO (*Pbcm*, $a \simeq 5.9$ Å, $b \simeq 5.5$ Å, $c \simeq 4.8$ Å) and γ-WO_3 ($P2_1/n$, $a \simeq 7.3$ Å, $b \simeq 7.5$ Å, $c \simeq 7.7$ Å) is observed. During the first 10 s, as the reaction mixture heats to 750°C, WO_3 undergoes a series of structural phase transitions – $P2_1/n$ (γ) to *Pcnb* (β, $a \simeq 7.4$ Å, $b \simeq 7.6$ Å, $c \simeq 7.8$ Å) to *P*4/*ncc* (α, $a \simeq 5.3$ Å, $c \simeq 7.8$ Å) – which are known to occur between 300 and 350°C, and between 720 and 850°C (Vogt *et al.*, 1999), respectively. Crystalline PbO peaks disappear in tandem with the formation of crystalline products and an increase in diffuse scattering, either from disorder within the crystalline product or from a mixed PbO–WO_3 melt (pure PbO melts at 888°C and pure WO_3 melts at 1473°C). At 750°C, Rietveld refinement indicates that three phases are present: WO_3 (*P*4/*ncc*), the $PbWO_4$ product ($I4_1/a$) and an additional crystalline intermediate, which was determined to be Pb_2WO_5 (*C*2/*m* , $a \simeq 14.3$ Å, $b \simeq 5.9$ Å, $c \simeq 7.6$ Å, $\beta \simeq 114°$). The amount of WO_3 and Pb_2WO_5 decreased as the $PbWO_4$ product increased. The consumption of WO_3 and Pb_2WO_5 to form the $PbWO_4$ product occurs most rapidly in the early stages of reaction and gradually slows, with more than half the $PbWO_4$ product formed within the first 30 s.

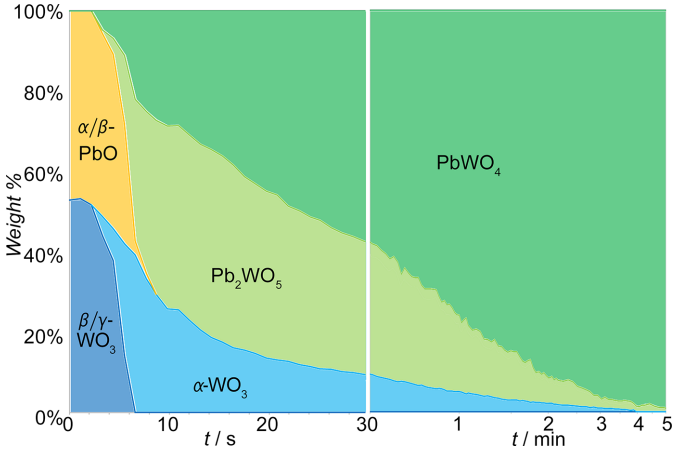

Figure 1
[Revised version of Fig. 6 of Hu *et al.* (2024).] Phase evolution during the reaction of PbO and WO_3 at 750°C within the RAPTR furnace, from Rietveld refinement of the time-resolved powder diffraction data.

After 5 min, peaks from $PbWO_4$ are observed as a near-phase-pure reaction product.

The Pb-rich intermediate Pb_2WO_5 phase observed here is a metastable, kinetic product which would most likely have been overlooked in conventional experiments (Jantz *et al.*, 2017). In this phase, lead oxide layers, consisting of edge- and face-sharing 7- and 9-coordinate polyhedra, are connected by WO_4 tetrahedra.

We note that the initial phase that forms, the Pb_2WO_5 phase, is richer in the lower valent, more mobile cation than the final product (*i.e.* Pb). That is, the Pb_2WO_5 intermediate has a higher Pb^{2+}:W^{6+} ratio than the $PbWO_4$ product. This may suggest that cations from the more mobile species diffuse or insert into other phases faster than they redistribute. This observation leads to pertinent questions on how the reaction kinetics and stoichiometry of intermediates depend on the relative mobility of ions within the target product.

Related literature. The following references are cited only in the supporting information: Bush *et al.* (2023), Coelho (2018), Dinnebier *et al.* (2018), Jantz *et al.* (2020), Kaurova *et al.* (2016), Moreau *et al.* (1996), Moreau *et al.* (1999), Takai *et al.* (2004), Tatsumi (1997), Triantafyllou *et al.* (1997), Wang *et al.* (2012), Zagorac *et al.* (2019).

Funding information

The following funding is acknowledged: US Department of Energy, Office of Science (award No. DE-SC0019212).

References

Bush, A. A., Kozlov, V. I., Stash, A. I. & Ivanov, S. A. (2023). *J. Struct. Chem.* **64**, 97–111.
Coelho, A. A. (2018). *J. Appl. Cryst.* **51**, 210–218.
Dinnebier, R. E., Leineweber, A. & Evans, J. S. O. (2018). *Rietveld Refinement: Practical Powder Diffraction Pattern Analysis Using TOPAS*. De Gruyter.
Hu, D., Beauvais, M. L., Mullens, B. G., Sanchez Monserrate, B. A., Vornholt, S. M., Kamm, G. E., Ferrari, J. J., Chupas, P. J. & Chapman, K. W. (2024). *J. Appl. Cryst.* **57**, 88–93.
Jantz, S. G., Pielnhofer, F., Dialer, M. & Höppe, H. A. (2017). *Z. Anorg. Allge Chem.* **643**, 2031–2037.
Jantz, S. G., Pielnhofer, F. & Höppe, H. A. (2020). *Z. Kristallogr. Cryst. Mater.* **235**, 311–317.
Kamm, G. E., Huang, G., Vornholt, S. M., McAuliffe, R. D., Veith, G. M., Thornton, K. S. & Chapman, K. W. (2022). *J. Am. Chem. Soc.* **144**, 11975–11979.
Kaurova, I. A., Kuz'micheva, G. M., Brykovskiy, A. A., Rybakov, V. B., Gorobets, Y. N., Shekhovtsov, A. N. & Cousson, A. (2016). *Mater. Des.* **97**, 56–63.
Moreau, J. M., Galez, P., Peigneux, J. P. & Korzhik, M. V. (1996). *J. Alloys Compd.* **238**, 46–48.
Moreau, J. M., Gladyshevskii, R. E., Galez, P., Peigneux, J. P. & Korzhik, M. V. (1999). *J. Alloys Compd.* **284**, 104–107.
Mullens, B. G., Nicholas, M. K., Marlton, F. P., Brand, H. E. A., Gu, Q., Maynard-Casely, H. E. & Kennedy, B. J. (2023). *J. Solid State Chem.* **321**, 123871.

Takai, S., Nakanishi, T., Oikawa, K., Torii, S., Hoshikawa, A., Kamiyama, T. & Esaka, T. (2004). *Solid State Ionics* **170**, 297–304.
Tatsumi, K. (1997). *Solid State Ionics* **96**, 35–40.
Triantafyllou, S. T., Christidis, P. C. & Lioutas, C. B. (1997). *J. Solid State Chem.* **130**, 176–183.
Vogt, T., Woodward, P. M. & Hunter, B. A. (1999). *J. Solid State Chem.* **144**, 209–215.
Wang, H., Chen, H.-H., Borrmann, H., Zhang, Z.-J. & Zhao, J.-T. (2012). *J. Alloys Compd.* **545**, 135–138.
Zagorac, D., Müller, H., Ruehl, S., Zagorac, J. & Rehme, S. (2019). *J. Appl. Cryst.* **52**, 918–925.